

Can A Universal Quantum Cloner Be Used to Design an Experimentally Feasible Near-Deterministic CNOT Gate ?

Amor Gueddana^{1,2}, Peyman Gholami¹ and Vasudevan Lakshminarayanan^{1,3}

1. Theoretical & Experimental Epistemology Lab, TEEL, School of Optometry and Vision Science, University of Waterloo 200 University Avenue West, Waterloo, Ontario N2L 3G1, Canada.
2. Green & Smart Communication Systems Lab, Gres'Com, Engineering School of Communication of Tunis, Sup'Com, University of Carthage, Ghazela Technopark, 2083, Ariana, Tunisia.
3. Department of Physics, Department of Electrical and Computer Engineering and Department of Systems Design Engineering, University of Waterloo 200 University Avenue West, Waterloo, Ontario N2L 3G1, Canada.

ABSTRACT

We propose a non-deterministic CNOT gate based on a quantum cloner, a quantum switch based on all optical routing of single photon by single photon, a quantum-dot spin in a double-sided optical microcavity with two photonic qubits, delay lines and other linear optical photonic devices. Our CNOT provides a fidelity of 78% with directly useful outputs for a quantum computing circuit and requires no ancillary qubits or electron spin measurements.

1. INTRODUCTION

Physical implementation of the photonic quantum computer and secure optical quantum communication systems are based on photonic quantum gates.¹ The gate which is universal for building all quantum circuits is the Controlled-NOT gate (CNOT).^{2,3} Experimentally realizable photonic CNOT gates are those based on linear optical devices.⁴⁻¹³ These gates have success probabilities less than 1/4. Further improvement in the success probability of this CNOT model is not possible because the best success probability for the CNOT functioning is 3/4 when using linear optical devices.¹⁴ This is a major hurdle for realization of all complex versions of the quantum computing circuits, since the success probability of such circuits may be very low due to multiple combinations of many non-deterministic CNOTs. To overcome this inefficiency, other techniques such as superconducting qubits¹⁵ have to be employed. Other work using non-linearities have been proposed in order to achieve non-deterministic CNOTs with high success probability.^{16,17} Other designs of CNOTs are based on spin of electron trapped in Quantum Dot (QD) and confined in a double sided optical micro-cavity.¹⁸⁻²² Although the fidelity values of these CNOTs seems to be near unity, in practice all these designs have major drawbacks. This is because of physical constraints that make them less effective in serial or parallel combinations. For the special CNOT model of Wang *et al.*,²⁰ we presented comments on the parametric values taken for the simulation and showed that the proposed CNOT gate is valid only in the strong coupling regime.²³ In this paper, we refer to this same CNOT and show that it provides a fidelity of only 47% in a realistic implementation (while it is 93.7% in the theoretical case), then we propose an optimized design based on a quantum cloner.

Several theoretical and experimental work has addressed quantum cloning machines providing optimal polarization cloning of single photons when using either Parametric Down Conversion (PDC) or photon bunching on Beam Splitter (BS). Fasel *et al.*²⁴ proposed close-to optimal quantum cloning of the polarization state of light using standard Erbium doped fiber for amplification and provided a fidelity F_{cloner} equal to 0.82. Linares *et al.*²⁵ proposed a cloning technique, based on stimulated emission in PDC using non linear β -Barium borate (BBo) crystal, and obtained experimental results with $F_{cloner} = 0.81$. Martini *et al.*²⁶ used for cloning a BBo crystal slab cut for type II phase matching for implementing optimal cloning and NOT gate. Bartuskova *et al.*²⁷ addressed in their work a phase covariant $1 \rightarrow 2$ qubit cloner based on two single mode optical fiber, non

linear crystal, attenuator and phase modulator, providing a fidelity of $F_{cloner} = 0.854$, which slightly surpasses the theoretical optimal value of the Universal Cloner (UC), denoted $F_{UC} = 5/6$. The question is: can these cloners be used for designing photonic CNOT gates? The main objective of this paper is to answer this question. Therefore, this paper is composed of five sections: Section 2 describes the several photonic components used for the CNOT design in the imperfect case. Section 3 presents the concept and modelling of the photonic CNOT using a quantum cloner and two quantum switches. In section 4, we present the simulation results and the corresponding experimental realization challenges. Finally, a conclusion is given in section 5.

2. IMPERFECT PHOTONIC DEVICES

Let us first consider the basic photonic components in the imperfect case as illustrated by figure 1.

Figure 1a illustrates a Half Wave Plate (HWP) with arbitrary error ξ . For inputs right-circularly polarized single photon denoted $|R\rangle$ and left-circularly polarized single photon denoted $|L\rangle$, the HWP behaves as follows:

$$|R\rangle \rightarrow \sqrt{\frac{1-\xi}{2}} |R\rangle + \sqrt{\frac{1+\xi}{2}} |L\rangle; |L\rangle \rightarrow \sqrt{\frac{1-\xi}{2}} |R\rangle - \sqrt{\frac{1+\xi}{2}} |L\rangle \quad (1)$$

An ideal Circular Polarizing Beam Splitter (CPBS) transmits $|R\rangle$ and totally reflects $|L\rangle$. When considering a CPBS with arbitrary errors τ_R and τ_L on $|R\rangle$ and $|L\rangle$, and for an arbitrary incident input state $\alpha|R\rangle + \beta|L\rangle$ (figure 1b), the CPBS transmits the state $\sqrt{\alpha - \tau_R}|R\rangle + \sqrt{\tau_L}|L\rangle$ and reflects the state $\sqrt{\tau_R}|R\rangle + \sqrt{\beta - \tau_L}|L\rangle$.

A quantum switch (SW) has two inputs I_1 and I_2 , and two outputs O_1 and O_2 . The transmittance (solid arrows in figure 1c) and reflectance (dashed arrows in figure 1c) coefficients from I_1 and I_2 to O_1 and O_2 , are denoted by $T_{1,2}$, $T_{2,1}$, $R_{1,1}$ and $R_{2,2}$. Several works addressed physical implementation of the quantum SW.²⁸⁻³¹ The switching process considered in this work is based on all optical routing of single photon by single photon, without any additional control field.³² This switch is based on three-level atomic Λ -configuration, with two different transitions denoted σ^+ and σ^- , and representing transitions coupled only to the right or to the left photonic mode propagation, respectively. Each of the inputs I_1 or I_2 , may be either transmitted or reflected into O_1 or O_2 , depending on the atom's state, being either on the $m_F = +1$ state or $m_F = -1$. When the atom is in this latter state, incoming photon on I_1 in the state σ^+ are reflected to O_1 and their state becomes σ^- , which toggles the atom's state to $m_F = +1$. When the atom's state is $m_F = +1$, it doesn't interact with σ^+ photons from I_1 and they are totally transmitted to O_2 . The whole process is symmetric for I_2 .

Other photonic devices used in our optimized model are the Beam Splitter (BS), the Quarter Wave Plate (QWP) and Delay Line (DL). In this work, we consider these devices only in the ideal case.

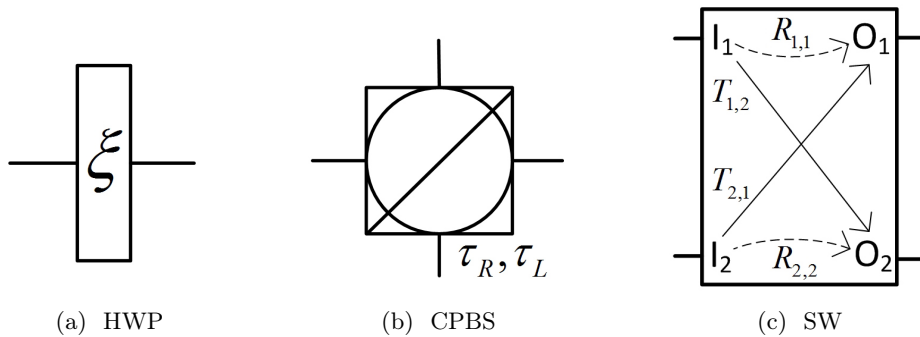


Figure 1: Photonic devices used for the design.

3. OPTIMIZED CNOT GATE MODEL BASED ON A QUANTUM CLONER

With the previously mentioned components, we propose a CNOT architecture using the quantum universal cloner as illustrated by figure 2.

The central part of the CNOT shaded grey is the proposed CNOT²⁰ under optimization. This CNOT is based on spin of electron in a QD trapped in a double sided optical microcavity which behaves like a BS.³³ Inside the grey background, we consider two input photons 1 and 2, being the control and target photons, with initial states $|\Psi_{ph}^1\rangle$ and $|\Psi_{ph}^2\rangle$, respectively.

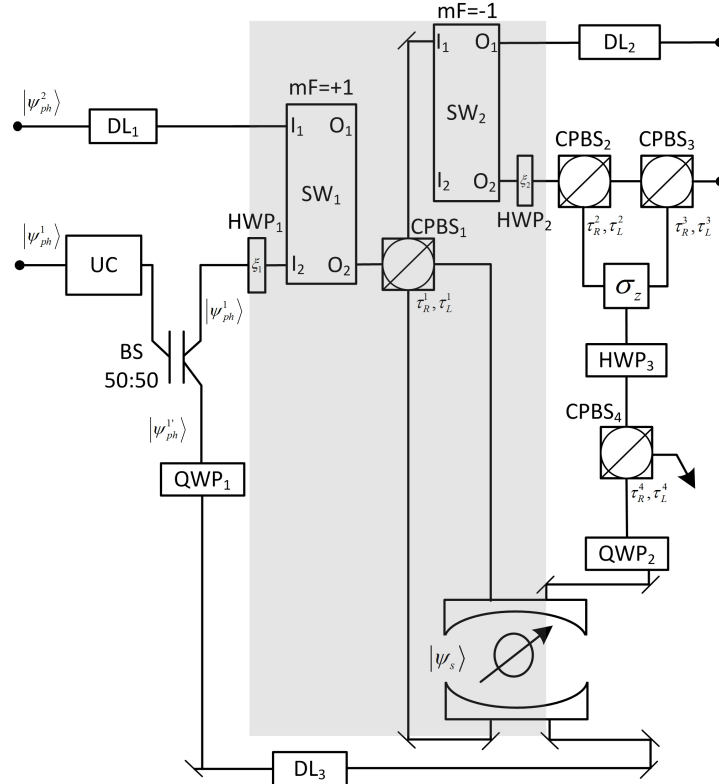


Figure 2: CNOT gate optimized model.

The electron spin state inside the QD is denoted $|\Psi_s\rangle$. Consider the following initial states:

$$\begin{aligned} |\Psi_{ph}^1\rangle &= \alpha |R_1\rangle + \beta |L_1\rangle \\ |\Psi_{ph}^2\rangle &= \delta |R_2\rangle + \gamma |L_2\rangle \\ |\Psi_s\rangle &= (|\uparrow_s\rangle - |\downarrow_s\rangle) / \sqrt{2} \end{aligned} \quad (2)$$

The two photons come successively to interact with the optical micro-cavity. For the coupled cavity, when considering equal the frequencies of the input photon, cavity mode and the spin-dependent optical transition, the reflection and transmission coefficients of the double sided optical micro-cavity system used in the CNOT design, are denoted $r(\omega)$ and $t(\omega)$, respectively, and are given by:^{20,22,33}

$$t(\omega) = -\frac{2\gamma\kappa}{\gamma(2\kappa + \kappa_s) + 4g^2}; \quad r(\omega) = 1 + t(\omega) \quad (3)$$

where g is the coupling strength, κ and $\kappa_s/2$ are the cavity field decay rate into the input/output modes and the leaky modes, respectively, and $\gamma/2$ is the X^- dipole decay rate. For the uncoupled cavity, the reflection and transmission coefficients are denoted $r_0(\omega)$ and $t_0(\omega)$, and they are directly obtained from equation 3 for $g = 0$. For a realistic spin cavity unit, the side leakage and cavity loss can not be neglected. In this case, $t(\omega)$ in the

coupled cavity and $r_0(\omega)$ in the uncoupled cavity will introduce bit-flip errors. Relevant energy levels and optical selection rules for exciton X^- inside the single charged GaAs/InAs QD, have been well detailed in,^{19,20} and the dynamics of the interaction of the QD spin in a double sided optical micro-cavity, for $r_0 = |r_0(\omega)|$, $t_0 = |t_0(\omega)|$, $r_1 = |r_1(\omega)|$ and $t_1 = |t_1(\omega)|$, are given as follows:

$$\begin{aligned}
|R^\downarrow, \uparrow_s\rangle &\rightarrow -t_0 |R^\downarrow, \uparrow_s\rangle - r_0 |L^\uparrow, \uparrow_s\rangle \\
|R^\downarrow, \downarrow_s\rangle &\rightarrow r_1 |L^\uparrow, \downarrow_s\rangle + t_1 |R^\downarrow, \downarrow_s\rangle \\
|R^\uparrow, \uparrow_s\rangle &\rightarrow r_1 |L^\downarrow, \uparrow_s\rangle + t_1 |R^\uparrow, \uparrow_s\rangle \\
|R^\uparrow, \downarrow_s\rangle &\rightarrow -t_0 |R^\uparrow, \downarrow_s\rangle - r_0 |L^\downarrow, \downarrow_s\rangle \\
|L^\downarrow, \uparrow_s\rangle &\rightarrow r_1 |R^\uparrow, \uparrow_s\rangle + t_1 |L^\downarrow, \uparrow_s\rangle \\
|L^\downarrow, \downarrow_s\rangle &\rightarrow -t_0 |L^\downarrow, \downarrow_s\rangle - r_0 |R^\uparrow, \downarrow_s\rangle \\
|L^\uparrow, \uparrow_s\rangle &\rightarrow -t_0 |L^\uparrow, \uparrow_s\rangle - r_0 |R^\downarrow, \uparrow_s\rangle \\
|L^\uparrow, \downarrow_s\rangle &\rightarrow r_1 |R^\downarrow, \downarrow_s\rangle + t_1 |L^\uparrow, \downarrow_s\rangle
\end{aligned} \tag{4}$$

Photon 1 first passes through HWP1, then it travels through the optical micro-cavity and then it passes through HWP2. The two switches used in the CNOT are denoted SW1 and SW2, the transmittance and reflectance coefficients of SW1 are denoted $T_{1,2}^1$, $T_{2,1}^1$, $R_{1,1}^1$ and $R_{2,2}^1$, while they are $T_{1,2}^2$, $T_{2,1}^2$, $R_{1,1}^2$ and $R_{2,2}^2$ for SW2. No details were given about SW1 and SW2 in,²⁰ and they were supposed to switch between photons 1 and 2 perfectly. After a certain time defined by DL1, photon 2 is switched by SW1 and injected to the spin cavity system, but before entering and after leaving the system, two Hadamard transforms are performed on the electron spin state, through $\pi/2$ microwave pulses,^{20,22} which transforms the state $|\uparrow_s\rangle \rightarrow (|\uparrow_s\rangle + |\downarrow_s\rangle)/\sqrt{2}$ and $|\downarrow_s\rangle \rightarrow (|\uparrow_s\rangle - |\downarrow_s\rangle)/\sqrt{2}$. After being switched by SW2, photon 2 is delayed by DL2 to wait for the interaction between photon 1 and its clone.

For the inputs of equation 2, the state at the output of the CNOT is then transformed as follows:

$$\begin{aligned}
&|\Psi_{ph}^1\rangle \otimes |\Psi_{ph}^2\rangle \otimes |\Psi_s\rangle \rightarrow \\
&(\alpha\delta |R_1\rangle |R_2\rangle + \alpha\gamma |R_1\rangle |L_2\rangle - \beta\delta |L_1\rangle |L_2\rangle - \beta\gamma |L_1\rangle |R_2\rangle) |\uparrow_s\rangle \\
&+ (\alpha\delta |R_1\rangle |R_2\rangle + \alpha\gamma |R_1\rangle |L_2\rangle + \beta\delta |L_1\rangle |L_2\rangle + \beta\gamma |L_1\rangle |R_2\rangle) |\downarrow_s\rangle
\end{aligned} \tag{5}$$

It is clear from equation 5 that the CNOT function is correctly entangled to the spin state $|\downarrow_s\rangle$, but a (-) sign is introduced to the CNOT when photon 1 is in the state $|L_1\rangle$ and both photons are entangled with the spin state $|\uparrow_s\rangle$. A measurement of the spin is required to determine the spin state, and then decide whether to apply an identity (I) or a negation gate (σ_z) on photon 1, to get correct CNOT entangled with both $|\uparrow_s\rangle$ and $|\downarrow_s\rangle$ states. This heralded function has a fidelity of 94 %, which means that the correct CNOT performed only with 47 % of success probability. However, without spin measurement, this CNOT model cannot be used in a serial or parallel combination, since the success probability of the entire circuit will decrease exponentially.

Our main idea is to eliminate this (-) sign at the output, in order to be independent of the spin state for further circuit realization. The idea is to apply a σ_z transform on photon 1, being at the state $|L_1\rangle$, only when the spin state at the output is $|\uparrow_s\rangle$. A measurement of the spin state inside a QD has been addressed in:³³ if we have an horizontally-polarized ($|H\rangle$) or vertically-polarized ($|V\rangle$) single photon at the input of QD spin system, being initially at the state $\mu |\uparrow_s\rangle + \nu |\downarrow_s\rangle$, it is possible using a QWP after the QD system to transmit the state of the electron to the photon as $\mu |R\rangle + \nu |L\rangle$. Based on this idea, we use in our architecture a UC to clone photon 1 and produce another photon 1' in the same state $|\Psi_{ph}^{1'}\rangle = |\Psi_{ph}^1\rangle = \alpha |R_{1'}\rangle + \beta |L_{1'}\rangle$. At the output of the UC, photon 1 and photon 1' are separated by a 50:50 BS. Photon 1 remains the control photon of the CNOT and photon 1' is created to be further used as control for the σ_z gate. After traversing QWP1, the state of photon 1' becomes $|\Psi_{ph}^{1'}\rangle = \alpha |H_{1'}\rangle + \beta |V_{1'}\rangle$. Photon 1' is then delayed by DL3 to wait for photons 1 and 2 to pass the QD system and alter the spin state (the spin state is initially given by equation 2, and after two imperfect Hadamard gates, it becomes $\mu |\uparrow_s\rangle + \nu |\downarrow_s\rangle$, for $\mu \approx \nu \approx 1/2$). Photon 1' passes through the QD spin system and after QWP2, its state becomes $|\Psi_{ph}^{1'}\rangle = \mu |R_1\rangle + \nu |L_1\rangle$. CPBS4 transmits $\mu |R_1\rangle$ while $\nu |L_1\rangle$ is discarded. The transmitted $\mu |R_1\rangle$ is flipped to $\mu |L_1\rangle$ by HWP3. At this level, photon 1' is present with same probability amplitude μ of the electron spin being at the state $|\uparrow_s\rangle$, moreover, it is exactly in the same mode of

photon 1, this allows it to serve as control for the σ_z gate. This gate should perform a $(-)$ sign only to photon 1 being at the state $|L_1\rangle$, this is the role of CPBS2 and CPBS3. Finally, the time interval between all photons, the paths lengths traveled by photons and the time delay of DL1, DL2 and DL3, should take into consideration cavity photon lifetime and single charged electron spin coherence time.²⁰

We consider ξ_1 and ξ_2 to be the errors related to HWP1 and HWP2. We suppose that $(\tau_R^1, \tau_L^1), (\tau_R^2, \tau_L^2), (\tau_R^3, \tau_L^3)$ and (τ_R^4, τ_L^4) are the errors related to CPBS1, CPBS2, CPBS3 and CPBS4, respectively. For simplicity, we neglect errors due to QWP1, QWP2 and HWP3. For the same inputs of equation 2, we compute the output of the optimized CNOT and we obtain:

$$\begin{aligned} & |\Psi_{ph}^1\rangle \otimes |\Psi_{ph}^2\rangle \otimes |\Psi_s\rangle \rightarrow \sqrt{T_{1,2}^1 R_{2,2}^1 T_{1,2}^2 R_{1,1}^2 F_{cloner}} \\ & \times ((\eta_1 |R_1\rangle |R_2\rangle + \eta_2 |R_1\rangle |L_2\rangle + \eta_3 |L_1\rangle |L_2\rangle + \eta_4 |L_1\rangle |R_2\rangle) |\uparrow_s\rangle \\ & + (\eta_5 |R_1\rangle |R_2\rangle + \eta_6 |R_1\rangle |L_2\rangle + \eta_7 |L_1\rangle |L_2\rangle + \eta_8 |L_1\rangle |R_2\rangle) |\downarrow_s\rangle) \end{aligned} \quad (6)$$

where:

$$\begin{aligned} \eta_1 = & \frac{\sqrt{1-\xi_2}}{2\sqrt{2}} \left((a_2 a_2' + a_4 a_4' - a_1 a_1' - a_3 a_3') (\delta \delta' + \gamma \gamma') + \right. \\ & \left. (a_2 a_2'' + a_4 a_4'' - a_1 a_1'' - a_3 a_3'') (\delta \delta'' + \gamma \gamma'') \right) \\ & a_1 = (\alpha + \beta) \sqrt{(1 - \tau_R^1)(1 - \xi_1)/2} \\ & a_2 = (\alpha + \beta) \sqrt{\tau_R^1(1 - \xi_1)/2} \\ & a_3 = (\alpha - \beta) \sqrt{(1 - \tau_L^1)(1 + \xi_1)/2} \\ & a_4 = (\alpha - \beta) \sqrt{\tau_L^1(1 + \xi_1)/2} \\ & a_1' = \sqrt{(1 - \tau_R^1)(t_0 + t_1) + (1 - \tau_L^1)(r_0 + r_1)} \\ & a_2' = \sqrt{\tau_R^1(t_0 + t_1) + \tau_L^1(r_0 + r_1)} \\ & a_3' = \sqrt{(1 - \tau_R^1)(r_0 + r_1) + (1 - \tau_L^1)(t_0 + t_1)} \\ & a_4' = \sqrt{\tau_R^1(r_0 + r_1) + \tau_L^1(t_0 + t_1)} \\ & a_1'' = \sqrt{(1 - \tau_R^1)(t_0 - t_1) + (1 - \tau_L^1)(r_0 - r_1)} \\ & a_2'' = \sqrt{\tau_R^1(t_1 - t_0) + \tau_L^1(r_1 + r_0)} \\ & a_3'' = \sqrt{(1 - \tau_R^1)(r_0 - r_1) + (1 - \tau_L^1)(t_0 - t_1)} \\ & a_4'' = \sqrt{\tau_R^1(r_1 + r_0) + \tau_L^1(t_1 - t_0)} \\ & \delta' = t_1 \tau_R^1 - t_0 (1 - \tau_R^1) \\ & \gamma' = r_1 \sqrt{\tau_R^1 \tau_L^1} - r_0 \sqrt{(1 - \tau_R^1)(1 - \tau_L^1)} \\ & \delta'' = t_1 (1 - \tau_R^1) - t_0 \tau_R^1 \\ & \gamma'' = r_1 \sqrt{(1 - \tau_R^1)(1 - \tau_L^1)} - r_0 \sqrt{\tau_R^1 \tau_L^1} \end{aligned} \quad (7)$$

and $\{\eta_i\}_{2 \leq i \leq 8}$ have all the same form of equation 7.

It is worth highlighting the fact that $\Theta = (-1) \times \sqrt{(1 - \tau_L^2)(1 - \tau_L^3)(1 - \tau_R^4)}$ is the operator that will eliminate the $(-)$ sign for the CNOT being entangled with $|\uparrow_s\rangle$, this operator appears only in η_3 and η_4 of equation 6. This is the main contribution in this work since the CNOT function is correctly entangled with both $|\uparrow_s\rangle$ and $|\downarrow_s\rangle$ spin states. To measure the performance of our optimized CNOT, we refer to the fidelity denoted F_{CNOT} and given by:²⁰

$$F_{CNOT} = \overline{\langle \Psi_{in} | U_{CNOT}^\dagger \rho_t U_{CNOT} | \Psi_{in} \rangle} \quad (8)$$

where the upper line indicates that the fidelity is obtained according to the average over all possible four input states $|\Psi_{in}\rangle$, U_{CNOT} is the ideal CNOT transform, $\rho_t = |\Psi_{out}\rangle \langle \Psi_{out}|$, with $|\Psi_{out}\rangle$ is the state at the output of the CNOT for the specific $|\Psi_{in}\rangle$ input.

4. SIMULATION RESULTS AND EXPERIMENTAL CHALLENGES

A first simulation concerns only the original proposed CNOT, where we study the impact of the errors of HWP1, HWP2 and CPBS1. To this end, we consider perfect SW1 and SW2 ($T_{1,2}^1 = T_{1,2}^2 = R_{2,2}^1 = R_{1,1}^2 = 1$), and we vary all errors around a realistic range of 10^{-2} .

We illustrate in figures 3a and 3b, the average fidelities for spin $|\uparrow_s\rangle$ and $|\downarrow_s\rangle$ states, denoted $\overline{F}_{CNOT}^\uparrow$ and $\overline{F}_{CNOT}^\downarrow$, versus the normalized coupling strength. Here we have set $\gamma = 0.1\kappa$.

In,²⁰ errors due to HWP1, HWP2 and CPBS1 have been neglected and it has been shown that the CNOT provides best $\overline{F}_{CNOT}^\uparrow$ or $\overline{F}_{CNOT}^\downarrow$ value around 93.74% for the strong coupling regime (obtained for $g > (\kappa_s + \kappa)/4$), and 32.34 % for the weak coupling regime (obtained when $g < (\kappa_s + \kappa)/4$). If we consider the same parameters used for the strong coupling ($\kappa_s = 0.05\kappa$ and $g = 2.5\kappa$) and weak coupling ($\kappa_s = 1.0\kappa$ and $g = 0.45\kappa$), our simulation shows that the errors affect the fidelities $\overline{F}_{CNOT}^\uparrow$ and $\overline{F}_{CNOT}^\downarrow$, and we obtain best values around 87.89% and 30.02%, respectively.

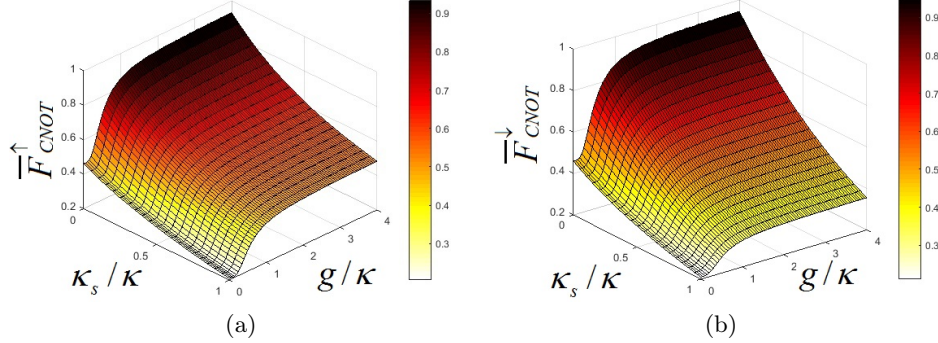


Figure 3: The average fidelity of the photonic CNOT gate versus the normalized coupling strengths κ_s/κ and g/κ . (a) The fidelity for electron spin in the state $|\uparrow_s\rangle$. (b) The fidelity for electron spin in the state $|\downarrow_s\rangle$.

Another simulation concerns our optimized model while taking into consideration realistic features of all devices. In this case, we consider SW1 and SW2 realized according to.³² For SW1 being initially in the state $m_F = +1$, the experimental results obtained are $T_{1,2}^1 = 89.9\%$, $R_{2,2}^1 = 65\%$. For SW2 being initially in the ground state $m_F = -1$, the obtained coefficients are $T_{1,2}^2 = 95.6\%$ and $R_{1,1}^2 = 64.8\%$. We consider the universal cloning of polarization state experimentally realized and providing $F_{cloner} = 0.82$.²⁴ We consider arbitrary errors around 10^{-2} affecting separately all devices of the CNOT of figure 2 (except QWP1, QWP2 and HWP3). With these assumptions, we show in Figure 4a the average fidelity of the CNOT function being correctly entangled with both $|\uparrow_s\rangle$ and $|\downarrow_s\rangle$, denoted $\overline{F}_{CNOT}^{\uparrow\downarrow}$. Best values according to figure 4a in the strong coupling regime is $\overline{F}_{CNOT}^{\uparrow\downarrow} = 26.27\%$.

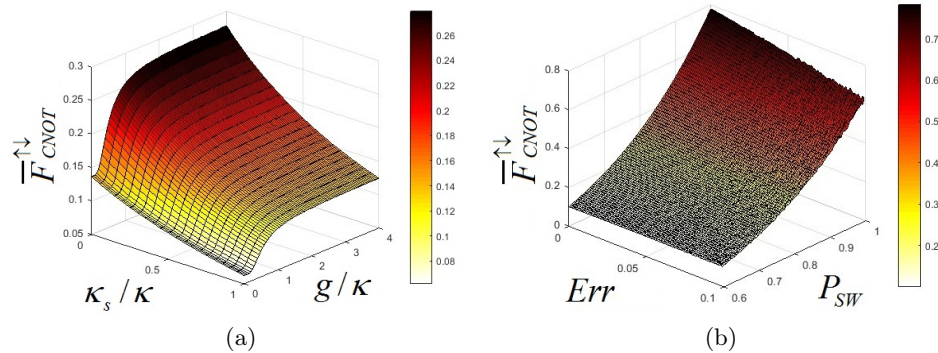


Figure 4: Simulation of the fidelity of the CNOT with realistic errors. (a) The average fidelity versus the normalized coupling strengths κ_s/κ and g/κ . (b) The average fidelity versus errors and success probability of the SWs.

It is clear that $\overline{F}_{CNOT}^{\uparrow\downarrow}$ value is highly sensitive to the fidelity of the cloner and SW1 and SW2 imperfections, we have considered only the strong coupling regime and the optimal cloner with $F_{UC} = 5/6$. We denote E_{rr} the set of all errors affecting the CNOTs components and we vary them in $[10^{-4}..10^{-1}]$. We consider also the same range of errors separately altering the coefficients $T_{1,2}^1$, $T_{1,2}^2$, $R_{2,2}^1$ and $R_{1,1}^2$, therefore, we denote $P_{SW} \simeq T_{1,2}^1 \simeq T_{1,2}^2 \simeq R_{2,2}^1 \simeq R_{1,1}^2$, and we illustrate $\overline{F}_{CNOT}^{\uparrow\downarrow}$ depending on E_{rr} and P_{SW} in figure 4b. The best fidelity permitted by our CNOT for lowest error range and P_{SW} approaching unity is $\overline{F}_{CNOT}^{\uparrow\downarrow}=78\%$. This fidelity is very close to F_{UC} and our optimized CNOT is very advantageous since neither a measurement of the electron spin state nor an extra treatment are required to allow using the CNOT outputs as inputs for another circuits.

5. CONCLUSION

We propose a quantum CNOT gate that overcomes the inefficiencies of a previously published CNOT design based on Quantum-Dot system. The previous proposal provides fidelity of 94 % but with a heralded functioning, which means that the correct CNOT performed only with 47 % probability success. Our CNOT functioning is not heralded by any spin states and it provides a success of 78%. This is a highly innovative result since it uses the quantum Cloner. This design will lead to another CNOT that uses the cloner with better fidelity approaching the cloner optimal limit of 5/6 and will allow possible generalization of the CNOT to all $C^m NOT$ photonic gates.

REFERENCES

1. P. Kok, W. J. Munro, K. Nemoto, T. C. Ralph, J. P. Dowling, and G. J. Milburn, "Linear optical quantum computing with photonic qubits," *Rev. Mod. Phys.* **79**, pp. 135–174, Jan 2007.
2. V. V. Shende, S. S. Bullock, and I. L. Markov, "Synthesis of quantum-logic circuits," *IEEE Transactions on Computer-Aided Design of Integrated Circuits and Systems* **25**, pp. 1000–1010, June 2006.
3. D. Maslov, G. W. Dueck, D. M. Miller, and C. Negrevergne, "Quantum circuit simplification and level compaction," *IEEE Transactions on Computer-Aided Design of Integrated Circuits and Systems* **27**, pp. 436–444, March 2008.
4. T. B. Pittman, B. C. Jacobs, and J. D. Franson, "Probabilistic quantum logic operations using polarizing beam splitters," *Phys. Rev. A* **64**, p. 062311, Nov 2001.
5. T. C. Ralph, N. K. Langford, T. B. Bell, and A. G. White, "Linear optical controlled-not gate in the coincidence basis," *Phys. Rev. A* **65**, p. 062324, Jun 2002.
6. J. L. O'Brien, G. J. Pryde, A. G. White, T. C. Ralph, and D. Branning, "Demonstration of an all-optical quantum controlled-not gate," *Nature* **426**, pp. 264 EP –, Nov 2003.
7. T. B. Pittman, M. J. Fitch, B. C. Jacobs, and J. D. Franson, "Experimental controlled-not logic gate for single photons in the coincidence basis," *Phys. Rev. A* **68**, p. 032316, Sep 2003.
8. S. Gasparoni, J.-W. Pan, P. Walther, T. Rudolph, and A. Zeilinger, "Realization of a photonic controlled-not gate sufficient for quantum computation," *Phys. Rev. Lett.* **93**, p. 020504, Jul 2004.
9. T. B. Pittman, B. C. Jacobs, and J. D. Franson, "Probabilistic quantum encoder for single-photon qubits," *Phys. Rev. A* **69**, p. 042306, Apr 2004.
10. X.-H. Bao, T.-Y. Chen, Q. Zhang, J. Yang, H. Zhang, T. Yang, and J.-W. Pan, "Optical nondestructive controlled-not gate without using entangled photons," *Phys. Rev. Lett.* **98**, p. 170502, Apr 2007.
11. A. S. Clark, J. Fulconis, J. G. Rarity, W. J. Wadsworth, and J. L. O'Brien, "All-optical-fiber polarization-based quantum logic gate," *Phys. Rev. A* **79**, p. 030303, Mar 2009.
12. A. Gueddana, M. Attia, and R. Chatta, "Non-deterministic quantum cnot gate with double encoding," *Proc.SPIE* **8875**, pp. 8875 – 8875 – 6, 2013.
13. A. Gueddana, A. Moez, and R. Chatta, "Abstract probabilistic cnot gate model based on double encoding: study of the errors and physical realizability," *Proc.SPIE* **9377**, pp. 9377 – 9377 – 8, 2015.
14. E. Knill, "Bounds on the probability of success of postselected nonlinear sign shifts implemented with linear optics," *Phys. Rev. A* **68**, p. 064303, Dec 2003.
15. J. H. Plantenberg, P. C. de Groot, C. J. P. M. Harmans, and J. E. Mooij, "Demonstration of controlled-not quantum gates on a pair of superconducting quantum bits," *Nature* **447**, pp. 836 EP –, Jun 2007.

16. M.-X. Luo, H.-R. Li, and H. Lai, "Quantum computation based on photonic systems with two degrees of freedom assisted by the weak cross-kerr nonlinearity," *Scientific Reports* **6**, pp. 29939 EP –, Jul 2016. Article.
17. C.-Y. Li, Z.-R. Zhang, S.-H. Sun, M.-S. Jiang, and L.-M. Liang, "Logic-qubit controlled-not gate of decoherence-free subspace with nonlinear quantum optics," *J. Opt. Soc. Am. B* **30**, pp. 1872–1877, Jul 2013.
18. H.-R. Wei and F.-G. Deng, "Scalable photonic quantum computing assisted by quantum-dot spin in double-sided optical microcavity," *Opt. Express* **21**, pp. 17671–17685, Jul 2013.
19. H.-R. Wei and F.-G. Deng, "Universal quantum gates on electron-spin qubits with quantum dots inside single-side optical microcavities," *Opt. Express* **22**, pp. 593–607, Jan 2014.
20. H.-F. Wang, J.-J. Wen, A.-D. Zhu, S. Zhang, and K.-H. Yeon, "Deterministic cnot gate and entanglement swapping for photonic qubits using a quantum-dot spin in a double-sided optical microcavity," *Physics Letters A* **377**(40), pp. 2870 – 2876, 2013.
21. M.-X. Luo and X. Wang, "Parallel photonic quantum computation assisted by quantum dots in one-side optical microcavities," *Scientific Reports* **4**, pp. 5732 EP –, Jul 2014. Article.
22. C. Bonato, F. Haupt, S. S. R. Oemrawsingh, J. Gudat, D. Ding, M. P. van Exter, and D. Bouwmeester, "Cnot and bell-state analysis in the weak-coupling cavity qed regime," *Phys. Rev. Lett.* **104**, p. 160503, Apr 2010.
23. A. Gueddana and V. Lakshminarayanan, "Comment on 'deterministic cnot gate and entanglement swapping for photonic qubits using a quantum-dot spin in a double-sided optical microcavity' by h.f. wang et al. [physics letters a 377 (2013) 2870-2876]," *Physics Letters A* , 2018.
24. S. Fasel, N. Gisin, G. Ribordy, V. Scarani, and H. Zbinden, "Quantum cloning with an optical fiber amplifier," *Phys. Rev. Lett.* **89**, p. 107901, Aug 2002.
25. A. Lamas-Linares, C. Simon, J. C. Howell, and D. Bouwmeester, "Experimental quantum cloning of single photons," *Science* **296**(5568), pp. 712–714, 2002.
26. F. D. Martini, D. Pelliccia, and F. Sciarrino, "Contextual, optimal, and universal realization of the quantum cloning machine and of the not gate," *Phys. Rev. Lett.* **92**, p. 067901, Feb 2004.
27. L. Bartůšková, M. Dušek, A. Černoč, J. Soubusta, and J. Fiurášek, "Fiber-optics implementation of an asymmetric phase-covariant quantum cloner," *Phys. Rev. Lett.* **99**, p. 120505, Sep 2007.
28. D. O'Shea, C. Junge, J. Volz, and A. Rauschenbeutel, "Fiber-optical switch controlled by a single atom," *Phys. Rev. Lett.* **111**, p. 193601, Nov 2013.
29. A. G. Smart, "A quantum switch routes photons one by one," *Physics Today* **67**, pp. 9–15, 2014.
30. S. Sun, H. Kim, G. S. Solomon, and E. Waks, "A quantum phase switch between a single solid-state spin and a photon," *Nature Nanotechnology* **11**, pp. 539 EP –, Feb 2016. Article.
31. T. Volz, A. Reinhard, M. Winger, A. Badolato, K. J. Hennessy, E. L. Hu, and A. Imamoglu, "Ultrafast all-optical switching by single photons," *Nature Photonics* **6**, pp. 605 EP –, Aug 2012.
32. I. Shomroni, S. Rosenblum, Y. Lovsky, O. Bechler, G. Guendelman, and B. Dayan, "All-optical routing of single photons by a one-atom switch controlled by a single photon," *Science* **345**(6199), pp. 903–906, 2014.
33. C. Y. Hu, W. J. Munro, J. L. O'Brien, and J. G. Rarity, "Proposed entanglement beam splitter using a quantum-dot spin in a double-sided optical microcavity," *Phys. Rev. B* **80**, p. 205326, Nov 2009.